Systematics of cluster decay modes

D. N. Poenaru
Advanced Science Research Center, Japan Atomic Energy Research Institute, Tokai, Ibaraki 319-1195, Japan;
National Institute of Physics and Nuclear Engineering, RO-76900 Bucharest, Romania;
and Institut für Theoretische Physik der J. W. Goethe Universität, D-60054 Frankfurt am Main, Germany

Y. Nagame*
Advanced Science Research Center, Japan Atomic Energy Research Institute, Tokai, Ibaraki 319-1195, Japan

R. A. Gherghescu
National Institute of Physics and Nuclear Engineering, RO-76900 Bucharest, Romania
and Institut für Theoretische Physik der J. W. Goethe Universität, D-60054 Frankfurt am Main, Germany

W. Greiner
Institut für Theoretische Physik der J. W. Goethe Universität, D-60054 Frankfurt am Main, Germany
(Received 13 January 2002; published 25 April 2002)

Spontaneous emission of some C, O, F, Ne, Mg, and Si isotopes, from heavy parent nuclei, have been experimentally observed since 1984, confirming earlier predictions. Experimental difficulties are mainly related to the low yield in the presence of a strong background of α particles. Until now, only some of the most favorable cases were investigated, leading to magic or almost magic proton and neutron numbers of daughter nuclei. We present a systematics of experimental results compared to calculations, clearly showing other possible candidates for future experiments. Universal curves may be used to estimate the expected half-lives.

DOI: 10.1103/PhysRevC.65.054308 PACS number(s): 23.70.+j, 27.90.+b

I. INTRODUCTION

A charged particle heavier than ^{4}He but lighter than a fission fragment is spontaneously emitted in a cluster decay mode of an atomic nucleus. There is a whole family of such disintegration modes: ^{14}C radioactivity, ^{24}Ne radioactivity, ^{28}Mg radioactivity, and so on. The first report on experimental discovery [1] and the theoretical predictions [2] are the two most cited papers in the field. Four theoretical models with predictive power were used in 1980: fragmentation theory, penetrability calculations as in the traditional theory of α decay, and numerical (NuSAF) and analytical (ASAF) superasymmetric fission models. Among the presented examples of potential barrier penetrability versus the mass and atomic numbers of emitted clusters from a given parent, those of ^{222}Ra and ^{224}Ra showed the best chance for ^{14}C to be emitted.

Despite some qualitative speculations expecting a larger yield for the stronger bound ^{12}C, the evidence of the ^{14}C radioactivity of ^{223}Ra was obtained at Oxford University in a brilliant experiment [1]. The determined values of the half-life, T, and branching ratio relative to the α decay, $b_\alpha = T_\alpha/T$, were confirmed by subsequently performed measurements.

A rapid development of experimental and theoretical investigations was stimulated by the discovery (see [3] and the references therein), and a new field was introduced in the Physics and Astronomy Classification Scheme (PACS): *23.70.+j Heavy-particle decay*.

The purpose of the present work is to present a systematics of experimental results compared to calculations, from which one may suggest other possible candidates for future experiments. Universal curves may be used to estimate the expected half-lives.

II. EXPERIMENTAL RESULTS

The main quantities experimentally determined are the partial half-life T and the kinetic energy of the emitted cluster, $E_k = QA_d/A$, where Q is the released energy, and A_d and A are the mass numbers of the daughter and parent nuclei. Usually the main experimental difficulties are caused by the very long half-lives and the small value of branching ratio relative to the α decay [4]. Sometimes the experimental sensitivity is not high enough to achieve a positive result; hence only an upper limit can be established. The longest upper limit determined up to now is $T \geqslant 10^{29.2}$ s for the ^{24,26}Mg radioactivity of ^{232}Th, and the smallest branching ratio $b_\alpha = 10^{-15.87}$ for ^{34}Si decay of ^{242}Cm. On the other hand, the most favorable values are $T = 10^{11.01}$ s for ^{14}C radioactivity of ^{222}Ra, and $b_\alpha = 10^{-8.88}$ for ^{14}C decay of ^{223}Ra.

An $\Delta E \times E$ telescope of two silicon detectors directly viewing the source was used in the first experiment [1], which ran six months in order to obtain 11 events. The strong background of α particles produced multiple pileups of electric pulses and damaged the semiconductor detectors which were replaced, after irradiation with about $10^9 \alpha/\text{cm}^2$, with new ones.

How does one get rid of these alphas? The solution adopted in the elegant experiments performed at Orsay was to deflect the unwanted ^{4}He ions, simply or doubly ionized,

*Email address: nagame@popsvr.tokai.jaeri.go.jp

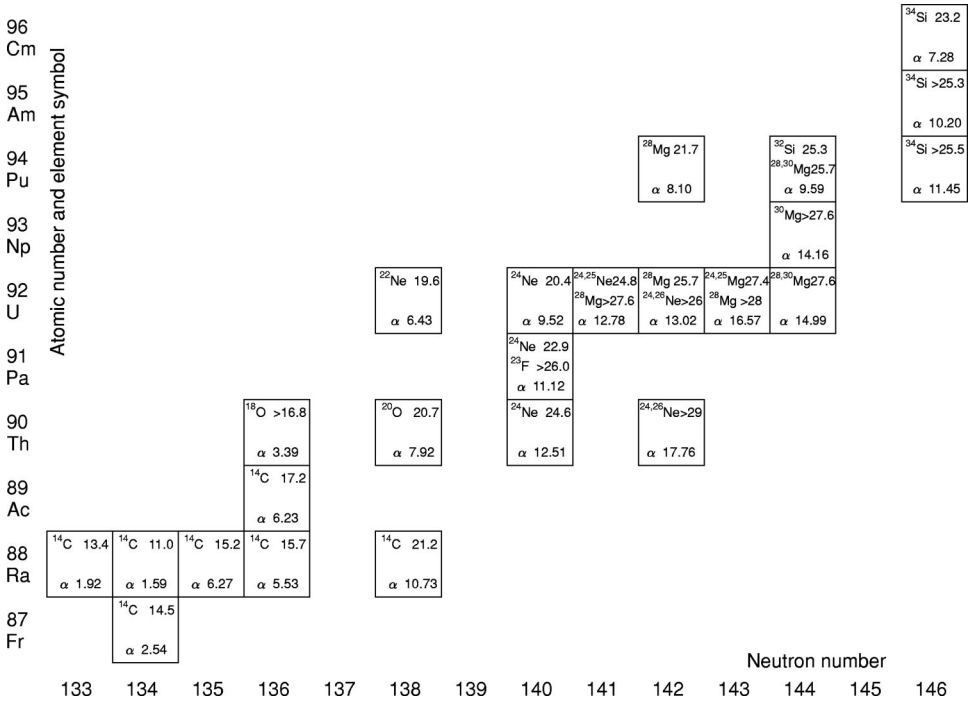

FIG. 1. Nuclear chart of experimentally determined cluster decay modes. The type of cluster decay, and the decimal logarithm of the half-life in seconds for cluster and α decay, is given for each parent nucleus with a specified proton and neutron number.

by a strong magnetic field produced in the superconducting spectrometer SOLENO, and to select only ^{14}C clusters to reach the detector in the focal plane. A source about 300 times stronger than that used by Rose and Jones was employed so that a run of only five days was necessary to obtain 11 events. With this unique instrument it was possible to discover [5] the fine structure in cluster decay [6], and to perform the most accurate experiment [7] by using high-quality implanted sources [8] of Ra isotopes made at the ISOLDE mass separator, CERN, Geneva. Similarly, an Enge split-pole magnetic spectrometer with a gas-filled detector in its focal plane was used at Argonne [9] to confirm the mass number of the emitted ^{14}C fragment from ^{223}Ra.

Another method extensively used [10,11] is based on solid-state nuclear track detectors (SSNTD's) [12,13] which are not sensitive to alphas and other low-Z particles, because they need a certain threshold of ionization. Very frequently such detectors are made from polyethylene terephtalate or from a phosphate glass. They are cheap and handy but, like photographic plates, do not deliver the information on line; only after a suitable post-irradiation chemical etching are the tracks visible. The etching rate along the paths of the ions depends on the charge number of the ionizing particle. The plot of the etching rate versus the residual range yields the atomic number, identification Z. Finally, the track can be seen, located, and measured by manual or automatic scanning with a microscope, and one may derive the characteristics of the incoming particle from its shape and dimensions. SSNTD's are widely used in a large variety of nuclear physics experiments, particularly for rare events in spontaneous fission, cold fission, and spontaneously fissioning shape isomers.

The data obtained until now (see Refs. [11,9,14,8,13], the references therein, and the recently published papers [15–18]) on half-lives and branching ratios of ^{14}C, ^{18,20}O, ^{23}F, $^{22,24-26}$Ne, ^{28,30}Mg, and ^{32,34}Si radioactivities are in good agreement with predicted values from the ASAF model, as we shall show below.

A summary may be seen in the nuclear chart (Fig. 1) in which the upper limits are marked with the mathematical sign $>$. When the experimental method did not discriminate between two neighboring isotopes of the emitted nucleus, both are mentioned with the same half-life. More than one cluster decay mode was detected for some isotopes of Pa, U, and Pu. The cluster emitters ^{221}Fr, $^{221-224,226}$Ra, ^{225}Ac, ^{228,230}Th, ^{231}Pa, $^{230,232-236}$U, ^{236,238}Pu, and ^{242}Cm are either β stable or not far from stability nuclei. The Green approximation for the line of β stability crosses the following Z,N pairs: 87,133; 88,135; 89,136; 90,138; 91,140; 92,142; 93,144; 94,146; 95,148; and 96,150. The α-decay half-lives are taken from tables of experimental data [4] when available, or otherwise calculated with a semiempirical formula [19].

The strong competition of α decay may be seen both from the numbers given in Fig. 1 and from the diagrams of Fig. 2 (in which the half-life T against cluster decay modes is denoted by T_c). While $10^{11}<T<10^{30}$ and $10^{1.5}<T_\alpha<10^{18}$, the branching ratio $10^{-16}<b_\alpha \equiv b_{\alpha c}=1/b_{c\alpha}<10^{-8}$.

Spontaneous fission [20] starts to be important in the region of heavy cluster emitters with $10^{14}<T_f<10^{26}$. For Pa, U, Np, Am, and Pu isotopes, the branching ratio $b_f=T_f/T \equiv b_{fc}=1/b_{cf}$ is in the range $(10^{-7},10^{2})$, but for ^{242}Cm it approaches 10^{-9}, making the measurement of ^{34}Si radioactivity very difficult [17,18]. On the right-hand side of Fig. 2 we plot the decimal logarithms $\log_{10} b_{c\alpha}$, $\log_{10} b_{cf}$, and $\log_{10} b_{f\alpha}=\log_{10}(T_f/T_\alpha)$.

Data for the *fine structure* of ^{14}C radioactivity of ^{223}Ra (see Refs. [8,3,21]) were not included because, surprisingly, the transition toward the first excited state of the daughter

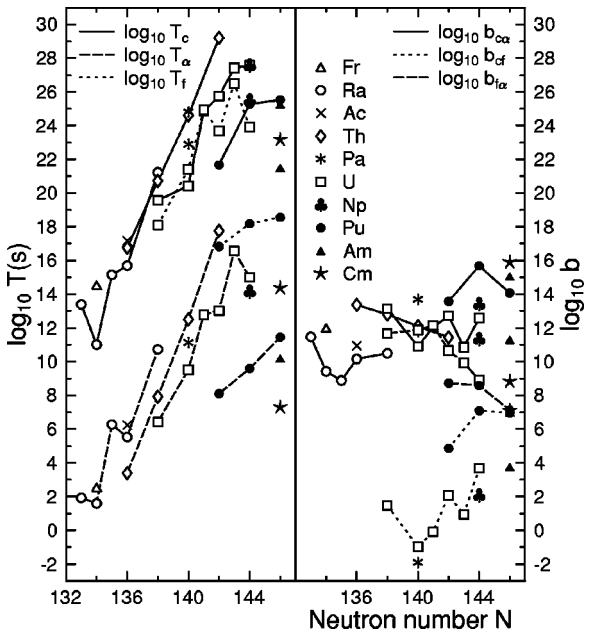

FIG. 2. Experimentally determined half-lives (left) and branching ratios (right) of heavy nuclei against cluster radioactivities, spontaneous fission, and α decay. Ths subscripts c, α, and f stand for cluster radioactivity, α decay, and spontaneous fission, respectively.

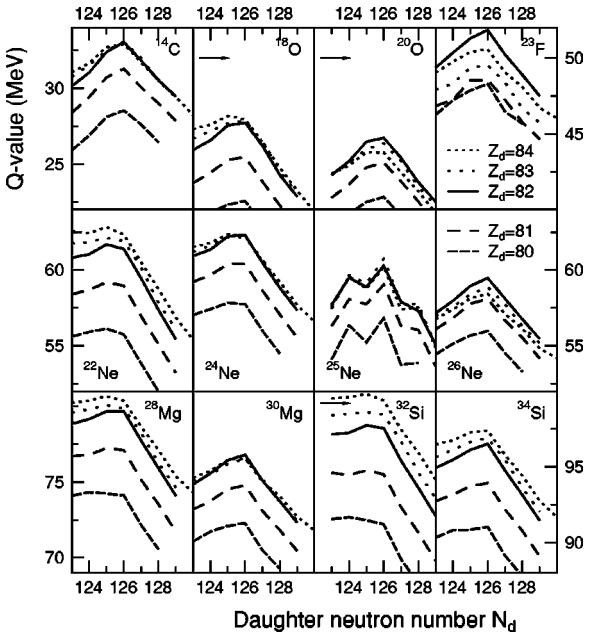

FIG. 3. Calculated Q values for different kinds of cluster decay modes vs the neutron number of the daughter nucleus. The points belonging to the same atomic number of the daughter are joined with a line of a style mentioned on the figure for $Z_d=80-84$.

nucleus is stronger than that to the ground state. The physical explanation for this relies on the nuclear structure of the parent and daughter nuclei. If the uncoupled nucleon is left in the same state in both the parent and heavy fragment, the transition is favored. Otherwise the difference in structure leads to a large hindrance $H=T^{exp}/T_{e\text{-}e}$, where T^{exp} is the measured partial half-life for a given transition, and $T_{e\text{-}e}$ is the corresponding quantity for a hypothetical even-even equivalent, estimated either from a systematics or from a model. A transition is favored if $H\simeq 1$, and it is hindered if $H>5$.

Unlike in α decay, where the initial and final states of the parent and daughter are not so different from one another, in cluster radioactivities of odd-mass nuclides, one has the unique possibility to study a transition from a well-deformed parent nucleus with complex configuration mixing, to a spherical nucleus with a pure shell model wave function. It can be used as a spectroscopic tool to obtain direct information on spherical components of deformed states. The interpretation of Ref. [22], according to which the main spherical component of the deformed parent wave function has an $i_{11/2}$ character, has been confirmed.

III. SHELL EFFECTS AND FUTURE MEASUREMENTS

The Q value is one of the quantities which play a very important role in any spontaneous nuclear decay with emission of charged particles. A parent nucleus with atomic and mass numbers A and Z decays into an emitted cluster A_e,Z_e and a daughter A_d,Z_d, ${}^{A}Z\rightarrow{}^{A_e}Z_e+{}^{A_d}Z_d$, with conservation of hadron numbers (neutrons and protons): $N=N_e+N_d$ and $Z=Z_e+Z_d$, where $A=N+Z$, and similar relationships for A_e and A_d. The process is energetically allowed if and only if the released energy

$$Q=M(A,Z)-[M_e(A_e,Z_e)+M_d(A_d,Z_d)] \qquad (1)$$

is a positive quantity, $Q>0$. The atomic masses M, M_e, and M_d, in units of energy, are taken from tables of experimental values [23].

Shell effects are clearly seen in Fig. 3, where we display Q values for the following decay modes: ^{14}C, ^{18,20}O, and ^{23}F (top), $^{22,24-26}$Ne (middle), and ^{28,30}Mg and ^{32,34}Si (bottom) versus the neutron number of the daughter, N_d. The points belonging to the same atomic number of the daughter are joined with a line of a style mentioned on the figure for $Z_d=80-84$.

The variation with the daughter neutron number N_d is almost regular giving, as a rule, a maximum value at the magic number $N_d=126$. Exceptions include ^{22,24}Ne, ^{28}Mg, and ^{32}Si decay modes with larger or equal values at $N_d=125$ or 124. Pairing effects are enhanced, leading to even-odd staggering for a cluster decay mode like ^{25}Ne (or ^{29}Mg which is not displayed). The variation with Z_d for $Z_d=80-82$ is, as expected, increasing toward the magic value $Z_d=82$, with an exception for ^{23}F radioactivity (almost the same values for $Z_d=80$ and 81). Only for ^{20}O and ^{26}Ne decay modes do Q values decrease when Z_d is increased past the magic number 82 ($Z_d=83$ and 84). For ^{23}F radioactivity $Z_d=84$ gives Q values smaller than $Z_d=82$ but higher than $Z_d=83$. They are very close to $Z_d=82$ for ^{14}C, ^{18}O, ^{24,25}Ne, and ^{30}Mg decay modes, but continue to increase slightly for ^{22}Ne, ^{28}Mg, and ^{32,34}Si radioactivity. These remarkable properties of high-Q values were not sufficiently exploited in

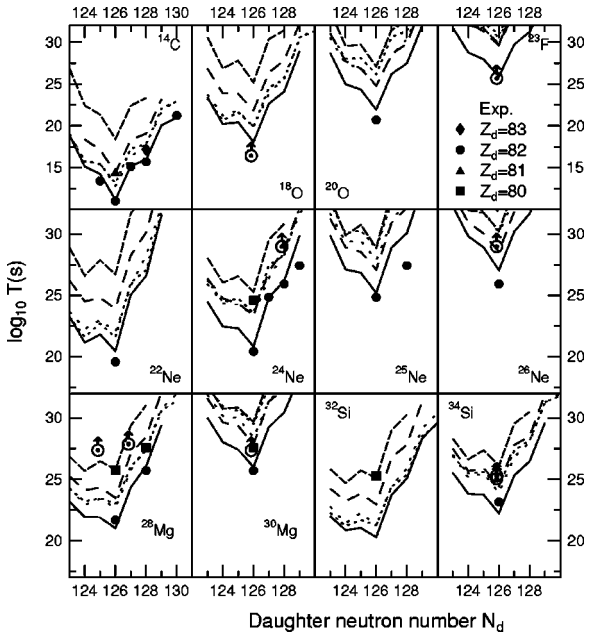

FIG. 4. Similar to Fig. 3 for predicted values within the ASAF model (lines) and experimentally determined (points) half-lives against different cluster decay modes vs the neutron number of the daughter. The line styles are the same as in Fig. 3 (e.g., continuous line for $Z_d=82$). The experimentally determined upper limits are marked with a vertical arrow. They correspond to $Z_d=82$ for ^{18}O and ^{23}F radioactivity, $Z_d=80$ for ^{24,26}Ne and ^{28}Mg radioactivity, and $Z_d=81$ for ^{30}Mg radioactivity. The two limits for ^{34}Si radioactivity refer to $Z_d=80$ (upper limit) and to $Z_d=81$ (lower limit).

practice up to now, as can be seen in Fig. 4, where a similar plot for the half-lives is shown, including the measured points.

A very large number of combinations of parent-emitted clusters had to be considered in a systematic search for new decay modes. In order to check the metastability of more than 2000 nuclides with measured masses [23] against about 200 isotopes of the elements with $Z_e=2-28$, this number is of the order of 10^5. The large amount of computations can be performed in a reasonable time by using an analytical relationship for the half-life. In 1980 the ASAF model was developed to fulfill this requirement. The Myers-Swiatecki liquid drop model potential barriers were adjusted with a phenomenological correction accounting for the known overestimation of the barrier height and for shell and pairing effects. Besides the half-life predictions in several papers, there are three large tables, two [24,25] published and one unpublished [26]. The predicted half-lives were used to guide the experiments.

A strong shell effect can be seen in Fig. 4: as a rule the shortest value of the half-life is obtained when the daughter nucleus has a magic number of neutrons ($N_d=126$) and protons ($Z_d=82$). There are few measurements of neighboring daughters with $Z_d=80$ or 81, and only one for $Z_d=83$. A striking exception is ^{32}Si decay, for which the single measurement performed until now is far from other more favorable cases.

Other possible candidates for future experiments, having reasonable half-lives and branching ratios relative to the α decay, could be ^{220,222,223}Fr, ^{223,224}Ac, and ^{225}Th as ^{14}C emitters; ^{229}Th for ^{20}O radioactivity; ^{229}Pa for the ^{22}Ne decay mode; ^{230,232}Pa, ^{231}U, and ^{233}Np for the ^{24}Ne radioactivity; ^{234}Pu for the ^{26}Mg decay mode; ^{234,235}Np and ^{235,237}Pu as ^{28}Mg emitters; and ^{238,239}Am and $^{239-241}$Cm for ^{32}Si radioactivity. Also the ^{31}Si decay of ^{241}Cm could be observed. One should not forget about the competition between spontaneous fission disintegration in Pu, Am, and Cm isotopes.

IV. PREFORMATION PROBABILITY AND UNIVERSAL CURVES

The (measurable) decay constant $\lambda=\ln 2/T$ can be expressed as a product of three (model-dependent) quantities

$$\lambda=\nu S P_s, \tag{2}$$

where ν is the frequency of assaults on the barrier per second, S is the preformation probability of the cluster at the nuclear surface, and P_s is the quantum penetrability of the external potential barrier. Not every quantity plays an equally important role. For α decay and cluster radioactivities the penetrabilty dominates the half-life variation with A. The frequency ν remains practically constant, the preformation differs from one decay mode to another but is not changed very much for a given radioactivity, while the general trend of penetrability closely follows that of the half-life. The external part of the barrier (for separated fragments), essentially of Coulomb nature, is much wider than the internal one (still overlapping fragments). Consequently, both fissionlike and α-like models, which take into consideration the external part of the barrier in the same manner, can provide a successful explanation for the measured half-lives. No wonder that the majority of cluster theories (see Refs. [3,27–29], and the references therein) are able to estimate the half-lives in good agreement with experiments. In fact the touching point is the scission configuration, which also proved to be very important for spontaneous and induced fission phenomena [30–32].

According to [33], the preformation probability can be calculated within a fission model as a penetrabilty of the internal part of the barrier, which corresponds to still overlapping fragments

$$S=\exp(-K_{ov}), \quad K_{ov}=\frac{2}{\hbar}\int_{R_a}^{R_t}\sqrt{2B(R)E(R)}dR, \tag{3}$$

where R_a is the internal turning point $[E(R_a)=0]$, $R_t=R_1+R_2$ is the separation distance of two fragments at the touching point configuration (scission), $B(R)$ is the nuclear inertia, and $E(R)$ is the deformation energy from which the Q value was subtracted out.

By taking into account the above-mentioned arguments, one may assume, as a first approximation, that preformation probability only depends on the mass number of the emitted cluster, A_e, in the following manner:

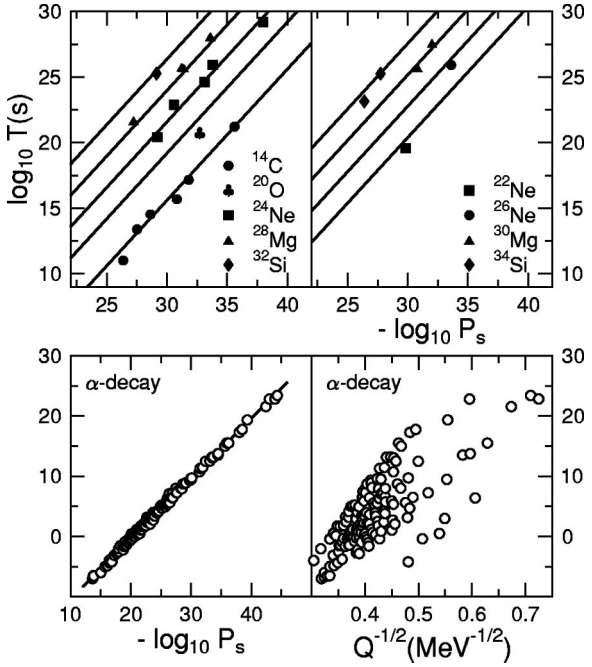

FIG. 5. Universal curves for cluster radioactivities (top left and right) and α decay (bottom left). In a typical "Geiger-Nuttal" plot for α decay (bottom right), one sees a considerable scattering of the data points.

$$\log S = \frac{(A_e - 1)}{3} \log S_\alpha , \tag{4}$$

where the preformation probability of the α particle S_α may be determined by a fit to experimental data. The next assumption is that $\nu(A_e, Z_e, A_d, Z_d) = \text{const}$. From the fit one obtains $S_\alpha = 0.0160694$ and $\nu = 10^{22.01}\ \text{s}^{-1}$.

In this way one arrives at a single straight line *universal curve* on a double logarithmic scale,

$$\log T = -\log P_s - 22.169 + 0.598(A_e - 1), \tag{5}$$

where

$$-\log P_s = c_{AZ}[\arccos\sqrt{r} - \sqrt{r(1-r)}], \tag{6}$$

with $c_{AZ} = 0.22873(\mu_A Z_d Z_e R_b)^{1/2}$, $r = R_t/R_b$, $R_t = 1.2249(A_d^{1/3} + A_e^{1/3})$, $R_b = 1.43998 Z_d Z_e / Q$, and $\mu_A = A_d A_e / A$. For all measurements performed up to now the agreement is good, as can be seen in Fig. 5. Usually a smooth behavior can only be obtained for even-even nuclei. Nevertheless, with one exception (the ^{14}C radioactivity of ^{223}Ra, for which the fine structure was observed), the measured parent nuclei with odd neutron or proton numbers were included on this plot, and they behave like the even-even nuclei.

Sometimes this universal curve is misinterpreted as being a Geiger-Nuttal plot. In 1911, Geiger and Nuttal found an empirical dependence of the α-decay partial half-life on the α-particle range in air. Nowadays this would correspond to a diagram of $\log T$ versus $Q^{-1/2}$. In this kind of systematics the experimental points are considerably scattered, as may be seen in Fig. 5 (bottom right) for the α decay of even-even nuclei.

Universal curves provide a means to obtain estimates of the expected half-lives rapidly. New searches for cluster decay modes can be made in the regions mentioned at the end of Sec. III.

ACKNOWLEDGMENTS

This research was supported by the Japanese Society for the Promotion of Science (JSPS), Tokyo, and by the Japan Atomic Energy Research Institute (JAERI), Tokai. One of us (D.N.P.) would like to acknowledge the hospitality during his research stage in Tokai.

[1] H. J. Rose and G. A. Jones, Nature (London) **307**, 245 (1984).
[2] A. Sǎndulescu, D. N. Poenaru, and W. Greiner, Fiz. Elem. Chastits At. Yadra **11**, 1334 (1980) [Sov. J. Part. Nucl. **11**, 528 (1980)].
[3] D. N. Poenaru and W. Greiner, *Nuclear Decay Modes* (Institute of Physics, Bristol, 1996), Chap. 6, pp. 275–336.
[4] A. Rytz, At. Data **47**, 205 (1991).
[5] L. Brillard, A. G. Elayi, E. Hourani, M. Hussonnois, J. F. Le Du, L. H. Rosier, and L. Stab, C. R. Acad. Sci. Paris **309**, 1105 (1989).
[6] M. Greiner and W. Scheid, J. Phys. G **12**, L229 (1986).
[7] E. Hourany *et al.*, Phys. Rev. C **52**, 267 (1995).
[8] E. Hourany, *Nuclear Decay Modes* (Ref. [3]), Chap. 8, pp. 350–369.
[9] W. Henning and W. Kutschera, *Particle Emission from Nuclei, Vol. II: Alpha, Proton and Heavy Ion Radioactivities* (CRC Press, Boca Raton, FL, 1989), Chap. 7, pp. 188–204.
[10] R. L. Fleischer, P. B. Price, and R. M. Walker, *Nuclear Tracks in Solids. Principles and Applications* (University of California, Berkeley, 1975).
[11] P. B. Price, Annu. Rev. Nucl. Part. Sci. **39**, 19 (1989).
[12] S. P. Tretyakova, Fiz. Elem. Chastits At. Yadra **23**, 364 (1992) [Sov. J. Part. Nucl. **23**, 156 (1992)].
[13] R. Bonetti and A. Guglielmetti, *Nuclear Decay Modes* (Ref. [3]), Chap. 9, pp. 370–392.
[14] E. Hourani, M. Hussonnois, and D. N. Poenaru, Ann. Phys. (Paris) **14**, 311 (1989).
[15] Qiangyan Pan *et al.*, Phys. Rev. C **62**, 044612 (2000).
[16] R. Bonetti, C. Carbonini, A. Guglielmetti, M. Hussonnois, D. Trubert, and C. Le Naour, Nucl. Phys. **A686**, 64 (2001).
[17] S. P. Tretyakova *et al.*, Radiat. Meas. **34**, 241 (2001).
[18] A. A. Ogloblin *et al.*, Phys. Rev. C **61**, 034301 (2000).
[19] D. N. Poenaru, M. Ivaşcu, and D. Mazilu, Comput. Phys. Commun. **25**, 297 (1982).
[20] D. C. Hoffman, T. M. Hamilton, and M. R. Lane, *Nuclear Decay Modes* (Ref. [3]), Chap. 10, pp. 393–432.
[21] M. Mirea and R. K. Gupta, *Heavy Elements and Related New Phenomena* (World Scientific, Singapore, 1999), Vol. II,

Chap. 19, p. 765.
[22] R. K. Sheline and I. Ragnarsson, Phys. Rev. C **55**, 732 (1997).
[23] G. Audi and A. H. Wapstra, Nucl. Phys. **A595**, 409 (1995).
[24] D. N. Poenaru, W. Greiner, K. Depta, M. Ivaşcu, D. Mazilu, and A. Sănd̆ulescu, At. Data **34**, 423 (1986).
[25] D. N. Poenaru, D. Schnabel, W. Greiner, D. Mazilu, and R. Gherghescu, At. Data **48**, 231 (1991).
[26] D. N. Poenaru, M. Ivaşcu, D. Mazilu, R. Gherghescu, K. Depta, and W. Greiner, Report NP-54, Central Institute of Physics, Bucharest, 1986.
[27] R. Blendowske, T. Fliessbach, and H. Walliser, *Nuclear Decay Modes* (Institute of Physics, Bristol, 1996), Chap. 7, pp. 337–349.
[28] R. G. Lovas, R. J. Liotta, A. Insolia, K. Varga, and D. S. Delion, Phys. Rep. **294**, 265 (1998).
[29] G. Royer and R. Moustabchir, Nucl. Phys. **A683**, 182 (2001).
[30] Y. Nagame, *et al.*, Phys. Lett. B **387**, 26 (1996).
[31] Y. L. Zhao, Y. Nagame, I. Nishinaka, K. Sueki, and H. Nakahara, Phys. Rev. C **62**, 014612 (2000).
[32] Y. L. Zhao *et al.*, Phys. Rev. Lett. **82**, 3408 (1999).
[33] D. N. Poenaru and W. Greiner, Phys. Scr. **44**, 427 (1991).